ISSN 1063-7834, Physics of the Solid State, 2006, Vol. 48, No. 8, pp. 1513–1520. © Pleiades Publishing, Inc., 2006.
Original Russian Text © L.A. Alekseeva, V.D. Natsik, R.V. Romashkin, L.A. Vashchenko, A.S. Garbuz, V.Yu. Lyakhno, 2006, published in Fizika Tverdogo Tela, 2006, Vol. 48, No. 8, pp. 1428–1435.

DEFECTS, DISLOCATIONS, AND PHYSICS OF STRENGTH

Plasticity and Strength of Nitrogen-Doped Normal-Hydrogen (n-H_2) Crystals

L. A. Alekseeva, V. D. Natsik, R. V. Romashkin, L. A. Vashchenko, A. S. Garbuz, and V. Yu. Lyakhno

Verkin Institute of Low-Temperature Physics and Engineering, National Academy of Sciences of Ukraine, pr. Lenina 47, Kharkov, 61103 Ukraine

e-mail: alekseeva@ilt.kharkov.ua

Received August 23, 2005; in final form, October 13, 2005

Abstract—The plastic and strength properties of polycrystals obtained as a result of rapid crystallization of a $N_2 + n$-H_2 gas mixture were studied. Samples were stretched under low loads at liquid-helium temperatures. A qualitative difference was revealed between the strain–stress curves for polycrystals of a $N_2 + n$-H_2 mixture and pure n-H_2. It was established that the N_2 impurity leads to a substantial increase in the plasticity resource and to a small increase in the strength of normal hydrogen. The experimental results are interpreted assuming a two-phase structure of the mixed polycrystals (namely, the presence of fine N_2 crystallites in large n-H_2 crystallites). The specific features of the formation of dislocation ensembles in this heterogeneous polycrystal and the evolution of these ensembles during deformation are discussed.

PACS numbers: 62.20.–x, 67.80.–s

DOI: 10.1134/S1063783406080154

1. INTRODUCTION

Solid hydrogen is a representative of a unique group of crystalline solids called quantum crystals. These crystals are formed by weakly interacting particles of a small mass, namely, helium and hydrogen isotopes [1]. Contrary to all other crystals, they are characterized by a very high intensity of lattice vibrations even at a temperature $T = 0$ K. For example, the root-mean-square amplitude of zero-point oscillations normalized to the lattice parameter is 30% in helium isotope crystals and about 20% in solid H_2. The specific character of the molecular dynamics in the hydrogen crystal suggests that its physicomechanical properties (including plasticity) differ from the typical properties of traditional classical crystals [2, 3]. This assumption has been confirmed experimentally [1, 4]. Since the Debye temperature of the H_2 crystal (~120 K [1]) is high as compared to the solidification temperature (~14 K [5]), this crystal will exhibit specific properties over the entire region of existence of the hydrogen crystalline state.

There is one more circumstance with which additional specific features of the physicomechanical properties of hydrogen crystals are associated. Normal hydrogen is a mixture of two molecular modifications in which the spins of the protons in a hydrogen molecule are either parallel to each other (orto-H_2, or o-H_2) or antiparallel (para-H_2, or p-H_2) [6]. The transitions between these states occur very rarely due to the weakness of the interaction of the nuclear spins with external fields. Thus, these two molecular modifications can be considered as two materials with different properties that are mutually soluble in any ratio. The main difference between them is that the o-H_2 molecules are ellipsoids of revolution and have a quadrupole moment; therefore, these molecules interact not only via van der Waals forces but also via electrostatic forces. In normal hydrogen (n-H_2), the contents of o-H_2 and p-H_2 are in a ratio of 3 : 1 [6]. Due to the presence of the orthohydrogen, the quantum properties of crystalline n-H_2 are less pronounced than those of crystalline parahydrogen.

The plastic and strength properties of hydrogen crystals are very sensitive to the contents of o-H_2 molecules [7, 8] and similar ellipsoidal molecules HD and D_2 [8, 9]. The presence of these modifications in parahydrogen even in small proportions (~0.2%) causes significant hardening and embrittlement of the samples. A peculiarity of another type has been revealed for hydrogen doped with inert-gas atoms. For example, the plasticity of an n-H_2 crystal has been observed to increase substantially due to the presence of ~0.010–0.001 at % Ne [10]. The anomalous plasticization of n-H_2 crystals caused by neon impurity indicates a complex and ambiguous character of the effect of impurities on the formation of low-temperature plastic and strength properties of hydrogen quantum crystals. In this connection, it is of interest to study in more detail the effects of other types of atomic and molecular impurities on the low-temperature plasticity of crystalline hydrogen.

Molecular nitrogen (N_2) is an interesting impurity for a hydrogen crystal. N_2 molecules have a relatively large mass and a lower zero-point oscillation intensity in a crystal than that of H_2 molecules. The presence of N_2 molecules in crystalline hydrogen can significantly decrease the probability of possible tunneling and band processes [2, 3] and the intensity of quantum fluctuations [8, 11–13] in the mobility of microdefects (vacancies, dislocation kinks, etc.) that are favorable for the deformation of hydrogen crystals. Moreover, the N_2 + H_2 system, like the Ne + n-H_2 system, is characterized by a sufficiently great difference between the values of the molar volumes of the impurity and hydrogen matrix. At $T = 0$ K, the molar volume of N_2 is 27.13 cm^3/mol, whereas the molar volume of H_2 varies within the limits 22.82–23.06 cm^3/mol depending on the orthohydrogen content [4]. Therefore, the plasticity of the $N_2 + H_2$ system can differ noticeably from that of n-H_2 due to the action of nitrogen molecules as dilatation centers, which can promote the nucleation of dislocations and hamper their motion.

The specific features of the influence of the N_2 impurity on the n-H_2 crystal plasticity are also determined by the formation of strongly coupled $N_2(H_2)_n$ complexes. The N_2 and o-H_2 molecules are ellipsoids of revolution. Therefore, in a matrix consisting of spherically symmetric p-H_2 molecules, it is energetically favorable for them to form quadrupole $N_2(o\text{-}H_2)_n$ complexes similar to van der Waals complexes in helium [14–16] and hydrogen [17–19]. The presence of these complexes can also have a substantial effect on the nucleation and motion of dislocations. Thus, it is difficult to predict the character of the influence of N_2 on the hydrogen plasticity.

The first experiments performed on parahydrogen samples with the orthohydrogen content decreased to ~0.2% have revealed mainly a hardening effect of the molecular-nitrogen impurity and no signs of plasticization [20]. Samples with high orthohydrogen contents have not been studied experimentally. A sharp increase in the o-H_2 concentration should enhance the role of the quadrupole forces in the intermolecular interaction in hydrogen crystals, since, contrary to p-H_2 molecules, the N_2 and o-H_2 molecules produce an electric field. The electric field produced by a significant number of host molecules and all dopant molecules in the solid n-H_2 should lead to the occurrence of a quadrupole "coat" of orthohydrogen molecules around N_2 impurity molecules, which, in turn, can change the plasticity and strength of the crystal. With the above considerations in mind, we performed a comparative study of the plasticity of pure n-H_2 crystals and of 0.12 mol % N_2 + n-H_2 "mixed" polycrystals.

2. EXPERIMENTAL TECHNIQUE

Nitrogen–hydrogen crystals were obtained from the liquid phase after condensation of a 0.12 mol % N_2 + n-H_2 gas mixture. The n-H_2 gas was 99.999 mol % pure. The gaseous nitrogen used to prepare the mixture was separated above the liquid fraction and was additionally refined using special laboratory equipment; the nitrogen gas was 99.99 mol % pure. The gas mixture was directed to the glass ampoule of a cryostat; the ampoule was cooled by liquid helium [21]. Since molecular nitrogen has a significantly higher melting temperature ($T_m \approx 63.15$ K [1, 4]) than H_2, the nitrogen begins to crystallize even in the gaseous-hydrogen stream and falls out in the form of white flakes on the inner surface of the ampoule and in the form of a powder on the surface of crystallizing H_2. Since the equilibrium solubility of N_2 in hydrogen is extremely low (less than 10^{-6} mol % [5]), the conditions of N_2 + n-H_2 crystal growth were chosen such that the molecules of solid N_2 were crystallization centers for liquid n-H_2. In this case, the crystal growth rate (approximately 0.8–0.9 mm/min) was nearly twice the growth rate at which pure n-H_2 polycrystals were obtained [21, 22].

The low initial temperature of the ampoule provided a required curvature (concavity) of the sample crystallization front. When the crystallization front was flat, the nitrogen impurity was displaced to the upper layers of the melt as the crystal grew and the sample working portion remained impurity-free. The deformation parameters of these samples coincided with those for the pure n-H_2.

Using the great difference between the molecular weights of the mixture components and varying the intensity of the injected gas stream, the pressure of the gas in the ampoule, and the initial temperature of the cooled ampoule, we optimized the growth regime and the growth rate of the solid phase to prepare artificial nonequilibrium (specific) nitrogen–hydrogen polycrystals, which could not be prepared under natural growth conditions. The transparency of these crystals is significantly worse than that of pure n-H_2 samples. The N_2 + n-H_2 mixed polycrystals obtained have a milk-white shade, indicating the presence of trapped and "frozen-in" N_2 molecules, molecular complexes, and even crystallites in the hydrogen crystal. The mean value of the grain sizes in the N_2 + n-H_2 samples measured using an MBS-2 long-focus microscope was found to be 1.5–2.0 mm. Because of a low resolution during the observation of the grain boundaries in H_2, we likewise cannot exclude the existence of finer grains.

The samples were annealed at 10–11 K and held isothermally at the test temperature (1.75 to 4.20 K) for about 40–50 min. The samples were stretched at a given temperature in steps under small loads $\Delta\sigma$ (~2–10 kPa) at regular time intervals Δt (2–3 min) up to failure. The sample loading was performed using a finely adjusted balance with a sensitivity of ±200 mg. The hydrogen-

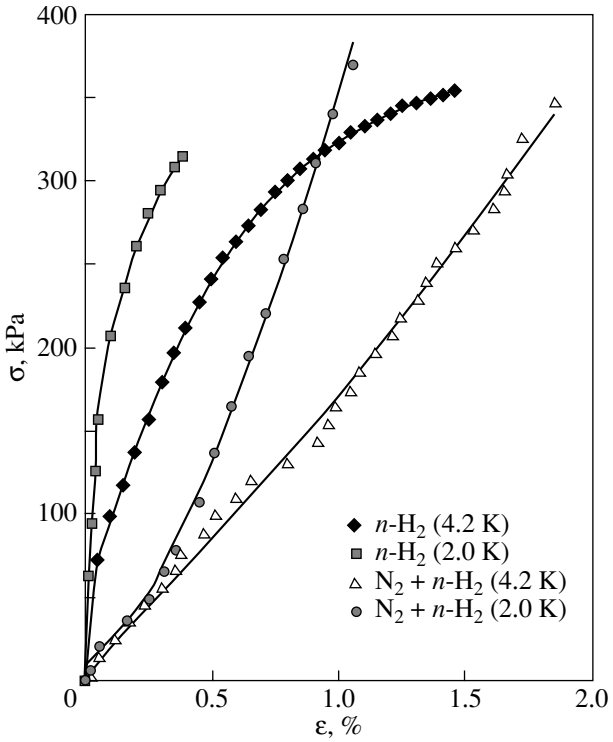

Fig. 1. Stress–strain curves for polycrystals of N_2 + n-H_2 mixtures and pure n-H_2 [22] obtained under equal loading conditions.

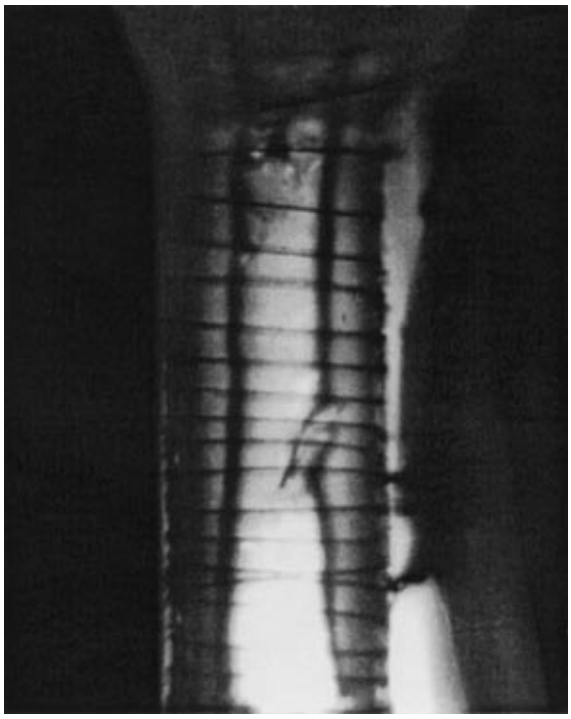

Fig. 2. View of a N_2 + n-H_2 mixed polycrystal immediately prior to fracture.

crystal length extension was measured accurate to $\pm 10^{-4}$ cm using an inductive displacement sensor [23]. The temperature was measured at the sample edges using two semiconductor resistance temperature detectors with an accuracy of $\pm 2 \times 10^{-2}$ K.

We took the fracture stress σ_f as a strength characteristic at a given temperature, and we took the ultimate strain ε_f achieved in the course of loading of a crystal up to its separation into parts as a characteristic parameter of plasticity. These quantities were determined from the $\sigma(\varepsilon)$ curves of the nitrogen–hydrogen samples studied.

3. EXPERIMENTAL RESULTS

Figure 1 shows the typical stress–strain curves (the dependences of the strain ε of the samples on the applied stress σ) measured at temperatures of 2 and 4.2 K and characterizing the plastic properties of the nitrogen–hydrogen mixed crystals under stepped loading. For comparison, the $\sigma(\varepsilon)$ curves obtained during analogous loading of pure n-H_2 samples are also shown [22]. The maximum stresses in these curves correspond to the sample fracture, whose initial stage is shown in Fig.2. It is seen from Fig. 1 that the H_2 polycrystals, as well as other polycrystals, do not have a pronounced yield strength, since the stress–strain curves for them do not exhibit a well-defined transition from the elastic to plastic region.

The effect of the nitrogen impurity on the parameters of the n-H_2 low-temperature deformation is ambiguous. If the fracture stress σ_f, which is the ratio of the maximum load to the final cross-sectional area of the sample, is taken to be the strength parameter, then, as is the case with p-H_2 [20], the nitrogen causes a relatively weak hardening of the n-H_2 samples (see table). In this case, indications of a softening (plasticizing) action of the impurity are also observed: first, the strain-hardening coefficients $d\sigma(\varepsilon)/d\varepsilon$ in the small-strain region for the N_2 + n-H_2 samples are significantly lower than those for the pure n-H_2 samples, and, second, the nitrogen impurity increases the maximum uniform strain ε_f, because the strain-hardening effect is small at the initial stage of deformation.

The stress–strain curves for both materials have initial stages of nearly linear hardening (at $\sigma < \sigma_0$). The critical load σ_0 and the corresponding strain ε_0 depend on the sample test temperature (see table), and they increase substantially as the temperature increases from 2.0 to 4.2 K. However, as seen from Fig. 1, there is a qualitative distinction between the $\sigma(\varepsilon)$ curves for polycrystalline nitrogen–hydrogen mixtures and pure n-H_2. Indeed, in the case of the pure n-H_2, the strain-hardening coefficient $d\sigma/d\varepsilon$ decreases monotonically as σ increases above σ_0, whereas in the N_2 + n-H_2 samples this coefficient increases with stress above σ_0.

Parameters of the stress–strain curves for polycrystals of pure n-H_2 (according to [22]) and N_2 + n-H_2 mixtures at 2 and 4.2 K

T, K	n_1	n_2	σ_0, kPa	ε_0, %	σ_f, kPa	ε_f, %	K_1, MPa	K_2, MPa
				$N_2 + n$-H_2				
2	0.82	1.51	63.44	0.329	368.84	1.06	19.28	41.78
4.2	0.92	1.21	130.98	0.801	345.81	1.84	16.35	20.68
				n-H_2				
2	0.95	0.59	181.30	0.10	323.40	0.24	129.79	9.12
4.2	0.80	0.40	198.94	0.31	352.80	1.40	18.64	1.96

It is known that, for most polycrystals, the strain-hardening $\sigma(\varepsilon)$ curves can be fitted by a power law $\sigma \sim \varepsilon^n$ [24]. In certain cases, over the entire strain range up to fracture, two or even more stages characterized by this power law with different values of n are observed. In [22], this power law was observed for pure n-H_2 polycrystals. An analysis of the $\sigma(\varepsilon)$ curves for the nitrogen–hydrogen mixed polycrystals showed (Fig. 1) that they have two stages characterized by the power laws

$$\sigma_1 = K_1\varepsilon^{n_1} \quad (\varepsilon < \varepsilon_0),$$

$$\sigma_2 = \sigma_0 + K_2(\varepsilon - \varepsilon_0)^{n_2} \quad (\varepsilon \geq \varepsilon_0).$$

The exponents n_1 and n_2, the coefficients K_1 and K_2, and the strain corresponding to the onset of the second stage ε_0 depend on the test temperature. By plotting the stress–strain curves in logarithmic coordinates, we determined the fitting parameters listed in the table. Note that the stress–strain curves for the nitrogen–hydrogen mixed polycrystals do not contain the "softening" stage characterized by $n = 0.5$; this stage is characteristic of the majority of polycrystals (including pure H_2 polycrystals [22]) and is commonly associated with quasi-static recovery processes [24].

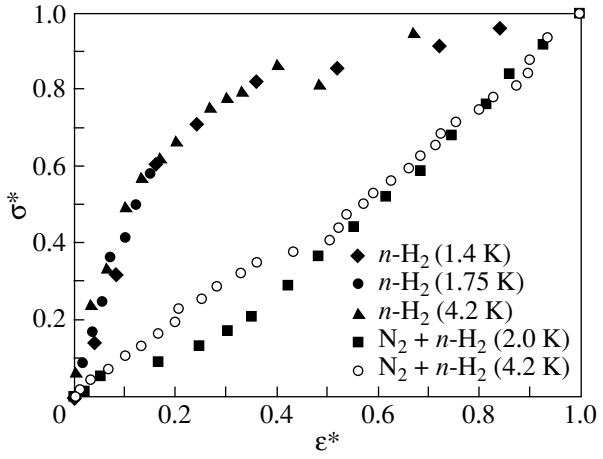

Fig. 3. Stress–strain curves for polycrystals of pure n-H_2 and N_2 + n-H_2 mixtures plotted in normalized coordinates.

The difference between the $\sigma(\varepsilon)$ curves for the N_2 + n-H_2 crystals and pure n-H_2 become even more noticeable when these curves are plotted in dimensionless coordinates equal to σ and ε normalized to the limiting stress σ_f and the limiting strain ε_f for each individual curve, respectively. Figure 3 shows the stress–strain curves obtained as a result of this normalization. It is seen from Fig. 3 that, in this representation, a specific law of temperature similarity is valid; namely, for each of the two materials studied, the stress-strain curves obtained at different temperatures practically coincide, but the curves for the pure n-H_2 polycrystals and for the N_2 + n-H_2 mixed polycrystals remain different. It should be noted that the temperature similarity of the stress–strain curves for the mixed polycrystals is somewhat violated at the initial stage of deformation.

An integrated study of polycrystals by the mechanical-test methods and of their morphology using transmission electron microscopy showed that, in many cases, the characteristics of the stress–strain curves, in particular, the parameters ε_f and σ_f, are immediately related to the dispersity (grain size) [24]. The grain boundaries in the hydrogen polycrystals are clearly distinguishable (Fig. 2), but in the literature there is no information on the influence of the grain size on the form and parameters of the stress–strain curves for n-H_2. To obtain this necessary information, we performed an additional investigation; namely, we tested eleven n-H_2 polycrystals of 99.999 mol % purity with larger grains (up to 2 nm in size) than in the earlier studies [7, 22]. Larger grains in n-H_2 formed at decreased crystallization rates (approximately 0.2–0.3 mm/min) and at higher initial temperatures of the ampoules in which the crystals were grown. In this case, the temperature of the cold finger near the bottom portion of an ampoule reached ~10 K. One of the stress–strain curves obtained in this case is shown in Fig. 4, which also shows the curve characteristic of the pure n-H_2 samples with finer grains. It is seen from Fig. 4 that a decrease in the grain size substantially increases the strain-hardening coefficient $d\sigma/d\varepsilon$ at all points of the stress–strain curve and significantly decreases the ultimate strain ε_f, whereas the change (increase) in the fracture stress σ_f of the n-H_2 polycrystals is significantly less. We also see that the shape of the $\sigma(\varepsilon)$ curves is the same for the two

values of the grain size of the n-H_2 polycrystals and in both cases differs significantly from the shape of the curves for the N_2 + n-H_2 mixed crystals (Fig. 1). This result suggests that the difference in plasticity between the pure n-H_2 polycrystals and N_2 + n-H_2 mixed polycrystals is caused by the effect of the nitrogen impurity not only on the dispersity of solid n-H_2 but also on other, more essential parameters of the crystals.

4. DISCUSSION OF THE EXPERIMENTAL RESULTS

From comparing the stress–strain curves for the N_2 + n-H_2 mixed and pure n-H_2 polycrystals (Figs. 1, 3, 4), it follows that, on the whole, the nitrogen impurity leads to a significant plasticization of the normal-hydrogen crystals. The plasticization effect is most pronounced at the initial stage of deformation (at $\varepsilon \leq 0.3\%$), where the strain-hardening coefficient $d\sigma/d\varepsilon$ for the mixture is approximately 10 times lower than that for pure hydrogen. This circumstance eventually causes a significant (by a factor of 2 to 3) increase in the plasticity resource, i.e., the ultimate fracture strain ε_f, but the fracture strengths σ_f for both materials differ insignificantly.

At the second deformation stage, the hardening effect of the nitrogen impurity is observed: here, the strain-hardening coefficient $d\sigma/d\varepsilon$ for the mixed polycrystals is noticeably higher than that for the pure hydrogen.

Another specific feature of the plasticity of the N_2 + n-H_2 mixed polycrystals is the weak sensitivity of the stress $\sigma(\varepsilon)$ to a variation in temperature at the first deformation stage for strains up to $\varepsilon = 0.3\%$. A thermally activated plastic flow of this material begins only at the second stage with an increase in the hardening effect.

In order to give a physical interpretation of these specific features, let us first discuss the specific features of the implantation of the N_2 molecular impurity into a hydrogen crystal lattice and the character of possible variations in the polycrystal morphology due to the impurity. Since the N_2 and o-H_2 molecules have the same symmetry, it appears reasonable that, in the hcp lattice of normal hydrogen, the configurations of these molecules and the symmetries of distortions created by them are similar. However, the gas-kinetic diameter of the N_2 molecule is 3.708 Å (see the Lennard–Jones parameters in [1, 4]), which is comparable to the nearest neighbor distance in n-H_2 hcp lattices (3.767 Å [1, 4]). Thus, individual N_2 molecules cause large local dilatations in the hydrogen lattice and can thereby influence the plastic-deformation processes. Indeed, the dilatation centers are strong obstacles to dislocation slip and, on the other hand, can stimulate the nucleation of mobile nonlinear excitations (kinks) on dislocations [25]. The former tendency decreases [24] and the latter

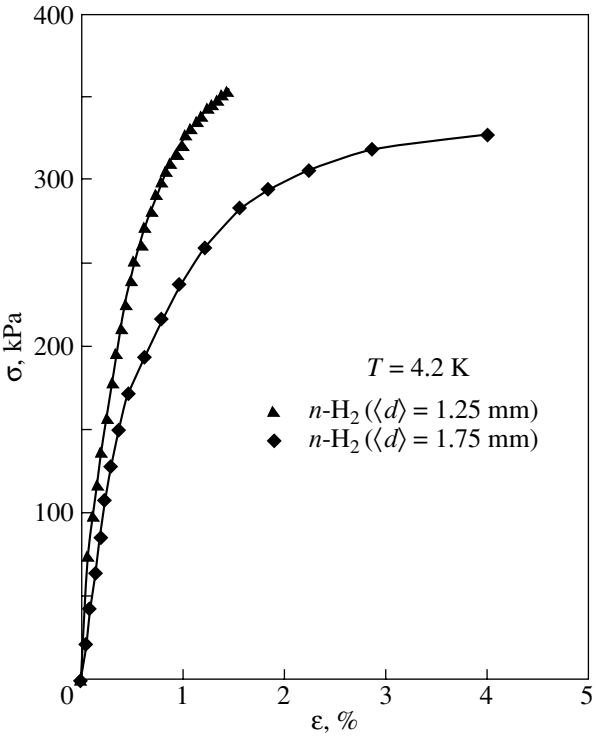

Fig. 4. Stress–strain curves for pure n-H_2 polycrystals with different dispersities.

increases [25] the plasticity of individual single-crystal fragments (grains) in the crystalline hydrogen.

When discussing the morphology of a solid N_2 + n-H_2 mixture, we should take into account the extremely low solubility of N_2 in solid H_2 [5], which excludes the formation of an equilibrium homogeneous solid solution of nitrogen in n-H_2 with the impurity concentration in question. Most likely, a two-phase nitrogen–hydrogen mixed crystal forms during the polycrystal growth. This assumption is supported by the results of the precise x-ray diffraction studies of N_2 + n-H_2 mixtures performed in [19], in which the effect of N_2 on the molar volume and identity periods of solid hydrogen were studied in detail. Indeed, beginning from the minimum nitrogen concentrations (1 mol %), the x-ray diffraction pattern showed sharp reflections characteristic of the usual crystalline phases formed by pure solid components (i. e., the reflections characteristic of the hcp or $Pa3$ structures of n-H_2 and the $Pa3$ structure of nitrogen, which is in the α phase at temperatures of 2.0 to 4.2 K).

Thus, it is conceivable that, in the course of growth of crystals of the N_2 + n-H_2 mixture, due to the extremely low solubility of nitrogen in solid hydrogen, heterogeneous mixed polycrystals most likely form, in which the softer hydrogen and hard nitrogen crystallites alternate. Note that the yield strength of nitrogen

crystals [4] exceeds that of normal-hydrogen crystals by a factor of 10 [7, 22].

There is another important factor that should be taken into account when considering the morphology of solid N_2 + n-H_2 mixtures, namely, the large difference between the values of the thermal expansion coefficients of hydrogen and nitrogen crystals. In the temperature range of interest, this coefficient for H_2 is nearly 6 times higher than that for N_2 [1, 4]. Therefore, when mixed polycrystals grow and the temperature varies during the growth, high thermoelastic stresses occur at the interfaces between N_2 crystallites and the n-H_2 matrix surrounding them. These stresses favor dislocation multiplication, above all, in more plastic n-H_2 crystallites.

The above specific features of the morphology of N_2 + n-H_2 mixed polycrystals and of their initial dislocation structure prior to the beginning of deformation determine the features of the plastic flow of these polycrystals observed in the experiment and the difference between the stress–strain curves for N_2 + n-H_2 and pure n-H_2 crystals.

The initial dislocation structure of the n-H_2 polycrystals seems to be similar to that of coarse-grained metallic polycrystals; namely, these crystals contain a system of growth dislocations distributed almost uniformly in individual grains. The onset and the first stage of plastic deformation in these polycrystals are associated with the motion of growth dislocations within individual grains and the formation of dislocation pileups at grain boundaries [24]. The ensemble formation determines the intensity of strain hardening at the first stage, where the hardening coefficient $d\sigma/d\varepsilon$ increases as the grain size decreases (Fig. 4). The temperature dependence of the stress at a constant strain $\sigma_\varepsilon(T)$ at the first stage is determined by the dislocation motion through Peierls barriers and impurity barriers inside grains. This motion occurs owing to thermal activation (at relatively high temperatures), quantum tunneling (at extremely low temperatures), or the joint action of thermal and quantum fluctuations (at intermediate temperatures) [8, 11–13]. Based on the available experimental data on the plasticity of pure n-H_2 polycrystals, we can conclude that the obstacles to dislocation slip in these crystals are mainly clusters (predominantly pairs) of o-H_2 molecules [26] and that dislocations overcome these obstacles at temperatures of 2.0 to 4.2 K owing to the joint action of thermal and quantum fluctuations. Only by substantially decreasing the o-H_2 concentration in hydrogen can one obtain very plastic coarse-grained polycrystals (or even single crystals) of pure p-H_2, for which the stress $\sigma_{\varepsilon(T)}$ is practically independent of temperature and the plastic flow has a quantum character [8, 27, 28]. This feature can be explained assuming that the obstacles to dislocation motion in pure p-H_2 crystals are mainly Peierls barriers and that they are overcome through the tunneling nucleation of pair kinks on dislocations [11]. A similar mechanism of plastic flow is operative in single crystals of certain pure metals [12, 29] at temperatures of the order of 1 K or lower.

It appears reasonable to assume that the transition to the second stage in the $\sigma(\varepsilon)$ curve for n-H_2 polycrystals is a consequence of the processes of "discharging" of dislocation pileups at grain boundaries; these processes are enhanced as the number of dislocations in pileups increases. Two discharge channels are the most probable: (i) the dislocation slip propagates through a grain boundary (dislocation "breakdown" of the boundary), and (ii) dislocations in ensembles leave their slip planes (climb) due to thermal and quantum diffusion of interstitial molecules and vacancies. These two discharge channels of dislocation pileups are microscopic mechanisms of decreasing the strain-hardening intensity at the second stage. In a phenomenological description of strain hardening, it is conventional to call processes of this type quasi-static recovery. These processes explain the shape of the $\sigma(\varepsilon)$ curves that are typical of coarse-grained polycrystals [24] and are observed upon deformation of pure n-H_2 polycrystals (Figs. 1, 4).

In a heterogeneous N_2 + n-H_2 mixed polycrystal, the mechanism of plastic deformation is different. First, it should be noted that, over the entire strain range up to sample fracture, the stress remains low as compared to the yield strength of N_2 crystallites [4]. Therefore, the crystallites themselves are not deformed but can influence the deformation process, because they can favor the dislocation multiplication in n-H_2 crystallites by acting as internal- (in particular, thermoelastic-) stress concentrators and can serve as obstacles to macroscopic dislocation flows in the slip direction. It is reasonable to assume that the plastic flow at the initial deformation stage is determined by the motion of dislocations in ensembles that formed in the n-H_2 crystallites during the crystallization of the mixture and temperature variations called for by the measurement procedure. These ensembles are in a substantially nonequilibrium state, and the initial deformation stage is associated with relatively small displacements of a great number of small fragments of dislocation lines, such as kinks and short segments located in the crystallite regions where the internal stresses act in the same direction as the applied stress. These processes occur either through purely mechanical (over-barrier) motion of the above-mentioned fragments of dislocation lines or due to a slight stimulating action of thermal and quantum fluctuations and are characterized by a low strain-hardening intensity and a weak temperature dependence of the stress. The initial deformation stage is completed with the depletion of the ensembles of nonequilibrium mobile fragments of the dislocation structure.

A further development of deformation requires the formation of macroscopic dislocation flows in relatively stable ensembles. Individual dislocations in the flows move through great distances and are forced to

overcome barriers created by o-H_2 molecules and individual N_2 molecules or $N_2(o\text{-}H_2)_n$ quadrupole complexes similar to those observed in [14–19], which are dissolved in a small proportion in the interior of n-H_2 crystallites. These barriers can be overcome mainly owing to the thermal activation, which explains the significantly increased stress and the increase in its sensitivity to temperature at the second deformation stage. At this stage, the N_2 crystallites act as insurmountable obstacles to dislocation flows in the n-H_2 matrix. These crystallites, as well as the grain boundaries in the n-H_2 polycrystal, favor the formation of dislocation pileups and their growth, which leads to an increase in the strain-hardening intensity. As noted above, as the stress increases, the dislocation pileups discharge at the boundaries between the n-H_2 crystallites, but the N_2 crystallites remain impenetrable to dislocations and cause the strain-hardening coefficient to increase up to sample fracture.

Thus, the specific features of the morphology of N_2 + n-H_2 mixed polycrystals determined by the low solubility of nitrogen in hydrogen, as well as the substantial difference in yield strength between the N_2 and n-H_2 crystals, allow us to qualitatively interpret all of the main regularities of the plastic deformation of this material revealed in the experiment.

5. CONCLUSIONS

In this work, the plastic deformation of polycrystals of nitrogen and normal hydrogen (0.12 mol % N_2 + n-H_2) mixture have been studied experimentally. The samples under study were prepared by rapid crystallization of mixtures at liquid-helium temperatures subjected to homogenizing annealing at a temperature of about 10 K. The measurement results have been compared with the experimental data obtained earlier in studying the plasticity of pure n-H_2 polycrystals [22].

The experiments have revealed an ambiguous influence of the N_2 impurity on the plasticity of normal-hydrogen polycrystals. The impurity has been observed to have a predominantly softening (plasticizing) effect. Indeed, at the initial deformation stage, the strain-hardening intensity of the N_2 + n-H_2 samples was significantly lower than that for the pure n-H_2 samples; the plasticity reserve (the ultimate uniform strain to fracture) is noticeably higher for the mixture samples. However, the impurity somewhat increases the ultimate strength of the polycrystals and substantially increases the strain-hardening intensity at the second deformation stage. Generally, the stress–strain curves for N_2 + n-H_2 mixed polycrystals and pure n-H_2 polycrystals are qualitatively different. Indeed, the stress–strain curves have a negative curvature (the strain-hardening coefficient decreases monotonically) for n-H_2 crystals and a positive curvature (the strain-hardening coefficient increases monotonically) for N_2 + n-H_2 mixtures.

The experimental data have been interpreted consistently assuming that the N_2 + n-H_2 mixed polycrystals have a heterogeneous structure; more specifically, during crystallization, fine N_2 crystallites form in the interior of larger n-H_2 crystallites due to the low mutual solubility of the mixture components. This morphology of the solid mixtures was revealed earlier in x-ray diffraction studies [19]. The great differences in the yield strength and thermal expansion coefficient between n-H_2 and N_2 crystallites cause the formation of a specific dislocation structure in the larger and more plastic n-H_2 crystallites, and the evolution of this structure during deformation determines the main specific features of the stress–strain curves for the mixed polycrystals.

ACKNOWLEDGMENTS

The authors are grateful to V.G. Manzhelii, A.I. Prokhvatilov, and K.A. Chishko for helpful discussions of the experimental results, A.V. Kuznetsov for her assistance in performing the experiment, and T.F. Lemzyakova for preparing the nitrogen–hydrogen gas mixtures and performing a chromatographic analysis of nitrogen and hydrogen.

REFERENCES

1. *Physics of Cryocrystals*, Ed. by V. G. Manzhelii, Yu. A. Freiman, M. L. Klein, and A. A. Maradudin (AIP, Woodbury, New York, 1996); V. G. Manzheliĭ and M. A. Strzhemechnyĭ, in *Cryocrystals*, Ed. by B. I. Verkin and A. F. Prikhot'ko (Naukova Dumka, Kiev, 1983) [in Russian].
2. A. F. Andreev and I. M. Lifshitz, Zh. Éksp. Teor. Fiz. **56**, 2057 (1969) [Sov. Phys. JETP **29**, 1107 (1969)]; A. F. Andreev, Usp. Fiz. Nauk **118**, 251 (1976) [Sov. Phys. Usp. **19**, 137 (1976)].
3. Yu. Kagan and L. A. Maksimov, Zh. Éksp. Teor. Fiz. **84**, 792 (1983) [Sov. Phys. JETP **57**, 459 (1983)].
4. A. I. Prokhvatilov, *Plasticity and Elasticity of Cryocrystals* (Begell House, New York, 2001).
5. B. N. Esel'son, Yu. P. Blagoĭ, V. N. Grigor'ev, V. G. Manzheliĭ, S. A. Mikhaĭlenko, and N.P. Neklyudov, *Properties of Liquid and Solid Hydrogen* (Izd. Standartov, Moscow, 1969; Israel Program for Scientific Translations, Jerusalem, 1971); B. I. Verkin, V. G. Manzhelii, V. N. Grigoriev, V. A. Koval', V. V. Pashkov, V. G. Ivantsov, O. A. Tolkacheva, N. M. Zvyagina, and L. I. Pastur, *Handbook of Properties of Condensed Phases of Hydrogen and Oxygen* (Hemisphere, New York, 1991).
6. A. Farkas, *Orthohydrogen, Parahydrogen, and Heavy Hydrogen* (Cambridge University Press, Cambridge, 1935; ONTI, Moscow, 1936).
7. D. N. Bol'shutkin, Yu. E. Stetsenko, and L. A. Indan, Fiz. Kondens. Sostoyaniya, No. 10, 86 (1970); Yu. E. Stetsenko, D. N. Bol'shutkin, and L. A. Indan, Fiz. Tverd. Tela (Leningrad) **12** (12), 3636 (1970) [Sov. Phys. Solid State **12** (12), 2958 (1970)].

8. I. N. Krupskiĭ, A. V. Leont'eva, L. A. Indan, and O. V. Evdokimova, Pis'ma Zh. Éksp. Teor. Fiz. **24** (5), 297 (1976) [JETP Lett. **24** (5), 266 (1976)].
9. L. A. Alekseeva, E. S. Syrkin, and L. A. Vashchenko, Fiz. Tverd. Tela (St. Petersburg) **45** (6), 1024 (2003) [Phys. Solid State **45** (6), 1073 (2003)].
10. L. A. Alekseeva, M. A. Strzhemechnyĭ, and G. N. Shcherbakov, Fiz. Nizk. Temp. **21** (9), 983 (1995) [Low Temp. Phys. **21** (9), 758 (1995)]; L. A. Alekseeva, M. A. Strzhemechnyĭ, and Yu. V. Butenko, Fiz. Nizk. Temp. **23** (4), 448 (1997) [Low Temp. Phys. **23** (4), 329 (1997)].
11. B. V. Petukhov and V. L. Pokrovskiĭ, Zh. Éksp. Teor. Fiz. **63** (2), 634 (1972) [Sov. Phys. JETP **36** (2), 336 (1973)].
12. V. D. Natsik and H.-J. Kaufmann, Phys. Status Solidi B **65**, 571 (1981).
13. I. N. Krupskii, A. V. Leontyeva, and Yu. S. Stroilov, Zh. Éksp. Teor. Fiz. **65** (5), 1917 (1973) [Sov. Phys. JETP **38** (5), 957 (1974)]; I. N. Krupskii, A. V. Leontyeva, Yu. S. Stroilov, and L. A. Indan, Fiz. Nizk. Temp. **1** (6), 749 (1975) [Sov. J. Low Temp. Phys. **1** (6), 360 (1975)].
14. E. B. Gordon, L. P. Mezhov-Deglin, and O. F. Pugachev, Pis'ma Zh. Éksp. Teor. Fiz. **19** (2), 103 (1974) [JETP Lett. **19** (2), 63 (1974)].
15. E. B. Gordon, L. P. Mezhov-Deglin, O. F. Pugachev, and V. V. Khmelenko, Chem. Phys. Lett. **54**, 282 (1978).
16. R. E. Boltnev, E. B. Gordon, I. N. Krushinskaya, A. A. Pel'menev, E. N. Popov, O. F. Pugachev, and V. V. Khmelenko, Fiz. Nizk. Temp. **18** (8), 819 (1992) [Sov. J. Low Temp. Phys. **18** (8), 576 (1992)].
17. A. S. Baryl'nik, A. I. Prokhvatilov, M. A. Strzhemechnyi, and G. N. Shcherbakov, Fiz. Nizk. Temp. **19**, 625 (1993) [Low Temp. Phys. **19** (5), 447 (1993)].
18. G. N. Shcherbakov, A. I. Prokhvatilov, M. A. Strzhemechny, and A. S. Barylnik, in *Proceedings of the Second International Conference on Cryocrystals and Quantum Crystals, Polanica-Zdroj, Poland, 1997* (Polanica-Zdroj, 1997), pp. 2–17.
19. N. N. Galtsov, A. I. Prokhvatilov, G. N. Shcherbakov, and M. A. Strzhemechny, Fiz. Nizk. Temp. **29** (9–10), 1036 (2003) [Low Temp. Phys. **29** (9), 784 (2003)].
20. L. A. Alekseeva and M. N. Kazeev, Preprint IAÉ-5299/7 (Kurchatov Institute of Atomic Energy), Moscow, 1991).
21. I. N. Krupskii, A. V. Leont'eva, L. A. Indan, and O. V. Evdokimova, Fiz. Nizk. Temp. **3** (7), 933 (1977) [Sov. J. Low Temp. Phys. **3** (7), 453 (1977)].
22. L. A. Alekseeva, O. V. Litvin, and I. N. Krupskii, Fiz. Nizk. Temp. **8** (2), 211 (1982) [Sov. J. Low Temp. Phys. **8** (2), 105 (1982)].
23. L. I. Danilenko, M. V. Zinov'ev, and V.A. Koval', Prib. Tekh. Éksp., No. 2, 212 (1973).
24. J. Friedel, *Dislocations* (Pergamon, Oxford, 1964; Mir, Moscow, 1967).
25. A. Sato and M. Meshi, Acta Metall. **21**, 753 (1973).
26. S. E. Kal'noi and M. A. Strzhemechnyi, Fiz. Nizk. Temp. **11** (8), 803 (1985) [Sov. J. Low Temp. Phys. **11** (8), 440 (1985)].
27. L. A. Alekseeva and I. N. Krupskiĭ, Fiz. Nizk. Temp. **10** (3), 327 (1984) [Sov. J. Low Temp. Phys. **10** (3), 170 (1984)].
28. L. A. Alekseeva, Candidate's Dissertation in Physics and Mathematics (Verkin Institute for Low Temperature Physics and Engineering of the National Academy of Sciences of Ukraine, Kharkov, 1986).
29. V. D. Natsik, G. I. Kirichenko, V. V. Pustovalov, V. P. Soldatov, and S. É. Shumilin, Fiz. Nizk. Temp. **22** (8), 965 (1996) [Low Temp. Phys. **22** (8) 740 (1996)].

Translated by Yu. Ryzhkov